

## Parametric investigation of factors affecting the behaviour of prismatic concrete specimens under high loading rates of uniaxial compressive loading

### Citation for published version:

Cotsovos, DM & Pavlovic, M 2006, 'Parametric investigation of factors affecting the behaviour of prismatic concrete specimens under high loading rates of uniaxial compressive loading', Paper presented at First South-East European Conference on Computational Mechanics, Kragujevac, Serbia and Montenegro, 28/06/06 - 30/06/06.

### Link:

[Link to publication record in Heriot-Watt Research Portal](#)

### Document Version:

Version created as part of publication process; publisher's layout; not normally made publicly available

### General rights

Copyright for the publications made accessible via Heriot-Watt Research Portal is retained by the author(s) and / or other copyright owners and it is a condition of accessing these publications that users recognise and abide by the legal requirements associated with these rights.

### Take down policy

Heriot-Watt University has made every reasonable effort to ensure that the content in Heriot-Watt Research Portal complies with UK legislation. If you believe that the public display of this file breaches copyright please contact [open.access@hw.ac.uk](mailto:open.access@hw.ac.uk) providing details, and we will remove access to the work immediately and investigate your claim.

## **Parametric investigation of factors affecting the behaviour of prismatic concrete specimens under high loading rates of uniaxial compressive loading**

**D. M. Cotsovos<sup>1</sup>, M. N. Pavlovic<sup>2</sup>**

<sup>1</sup> Concept Engineering Consultants  
8 Warple Mews, Warple Way, London W3 0RF, UK  
e-mail: dkotsovos76@yahoo.co.uk

<sup>2</sup> Department of Civil Engineering,  
Imperial College, London SW7 2AZ, UK  
e-mail: m.pavlovic@imperial.ac.uk

### **Abstract (150 - 450 words):**

This study investigates the response of structural concrete to high rates of loading. The research is based on a finite-element (FE) program capable of carrying out three-dimensional (3D) nonlinear static and dynamic analyses which has been found to be capable of yielding realistic predictions to the response of plain- and reinforced-concrete structures under arbitrary static and dynamic actions. The FE model incorporates a 3D material model of concrete behaviour which is characterized by both its simplicity (fully brittle, with neither strain softening nor load-path dependency) and its attention to the actual physical behaviour of concrete in a structure (unavoidable triaxiality prior to local material failure which is described on the basis of experimental data of concrete cylinders under definable boundary conditions). The most significant feature of this model under impact is that it is based on the use of static material properties of concrete, since it assumes that the effect of loading rate on the specimen behaviour can be attributed primarily to the inertia of the structure's mass and not, as is at present widely considered, to the loading-rate sensitivity of the material properties of concrete. The existing experimental data, used in order to validate the FE model presently adopted, are characterized by considerable scatter. When reviewing the details of the various experimental investigations carried out to date, it is apparent that a number of parameters (such as the static uniaxial compressive strength of concrete  $f_c$ , the experimental techniques used for the tests, the shape and size of the specimens, the density of concrete, etc) vary from one experiment to another. Thus, it is the aim of this article to use the FE model in order to investigate the individual and combined effects of these parameters on the response of plain-concrete prismatic specimens under high rates of uniaxial compressive loading and, in so doing, to identify the significance of their contribution to the overall scatter that characterizes experimental data.

**Key words:** loading-rate, dynamic, concrete, inertia, impact

## 1. Introduction

The application of an external load onto a concrete structural form leads to the development of a complex triaxial stress field within it which is further accentuated by its cracking processes and the ensuing internal stress redistributions [1]. In addition, if the loading is dynamic, stress waves propagate through the concrete medium. Their speed is directly linked to the material properties of concrete while their stress intensity level depends on the intensity of the imposed load. The formation of such waves affects the triaxial stress field and may cause the development of high stress concentrations in localised regions of the specimen leading to local failure/cracking. The complexity of the above stress field is further intensified by the fact that the stress waves may be deflected by voids formed due to the ongoing cracking process, as well as at the boundaries of the structural form under investigation. Clearly, the behaviour of concrete structural forms under dynamic – and especially high-rate – loading is a complicated nonlinear wave-propagation dynamic problem.

The FE package presently adopted is capable of carrying out three-dimensional (3D) nonlinear static and dynamic analyses. Its formulation is based on the hypothesis that material properties of concrete are independent of the rate of loading, thus relying for its response solely on the realistic description of the triaxial nonlinear behaviour of concrete under static loading as well as the effect of the inertia of the structure's mass. This program is known to yield realistic predictions to the response of a wide range of plain-and reinforced-concrete structural forms subjected to arbitrary static and earthquake actions, as well as of plain-concrete prisms under high rates of uniaxial compressive loading [1,2]. For the latter problem (i.e. impact), both numerical predictions and experimental data indicate that the application of high rates of uniaxial compressive loading on concrete prisms results in these specimens exhibiting high rates of axial and lateral deformation which, in turn, triggers the development of significant inertia forces. These forces have a confining effect on the prism and tend to restrict the deformations in both the axial and lateral directions, thus effectively slowing down the cracking procedure that the prism undergoes. This causes the prisms to exhibit higher load-carrying-capacities and maximum values of strains (compared to their counterparts tested under static loading) as loading rates increase. The good correlation between numerical predictions and available experimental data suggests that the change in the behaviour of the concrete prisms under high loading rates is primarily due to the inertia forces that develop during the loading process, and provides an alternative explanation regarding the causes that trigger the changes exhibited in the response of plain-concrete prisms under increasing loading rates as it does not rely on the presently (widely) accepted assumption of strain-rate sensitivity of the material properties of concrete.

Nevertheless, existing experimental data are characterized by considerable scatter and, in reviewing the dynamic tests carried out to date, one observes that a number of parameters vary from one experiment to another. Such parameters include the static uniaxial compressive strength of concrete ( $f_c$ ), the experimental techniques used for the tests, the shape and size of the specimens, and the density of the concrete. The available test data do not reveal to what extent variations of the above parameters affect the specimen response. This is mainly due to the lack of experimental data investigating the individual effect of each parameter, as well as the scatter that characterizes all existing data. However, the majority of these parameters are linked to the dynamic (structural) characteristics of the specimen/structure, such as the stiffness, the mass and the boundary conditions. Keeping in mind that the specimens used in tests must be viewed as structures, changes – even small ones – in the values of these various characteristics may (potentially) result in significant changes in the specimens' response under dynamic loading. The present article focuses on investigating, through numerical analysis, the effects that the variation of these various parameters have on specimen response and experimental scatter. One possible parameter that is not considered is high moisture content, since the material model corresponds to practical concrete which is usually air-cured, hence possessing low moisture content.

## 2. Experimental background

Over the past few decades a large number of experiments have been carried out on the behaviour of concrete (prismatic or cylindrical) specimens under high rates of uniaxial compressive loading (for a thorough bibliography of the copious laboratory data encompassing hundreds of tests see, for example, refs [2,3]. A summary of the available experimental data is presented in graphical form in Fig. 1 expressing the relationship between the load-carrying capacities of the specimen (with respect to its counterpart under static loading) and the exhibited axial strain-rate. The primary objective of such experiments is to investigate the behaviour of concrete at a material level under high-rate loading since the response of these specimens during the dynamic tests has been shown to differ considerably from that of their counterparts tested under static conditions. This difference primarily takes the form of an increase in the specimens' load-carrying capacity, a difference which becomes more apparent as the loading rate increases.

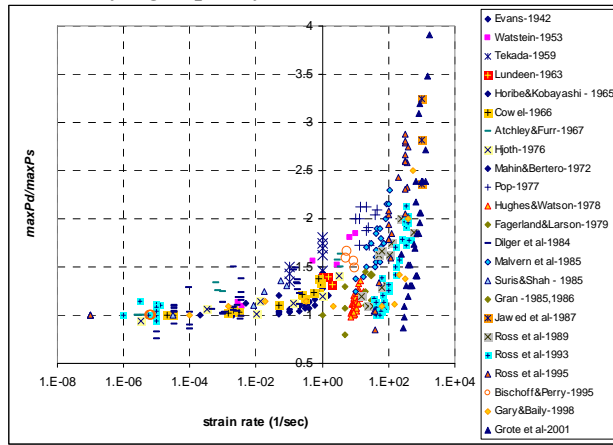


Figure 1. Variation of load-carrying capacity with strain rate for concrete in uniaxial compression ( $\max P_d$  = load carrying capacity,  $\max P_s$  = load-carrying capacity under static loading).

Although all the experimental investigations show that there is a definite link between the loading-rate and specimen response, the considerable scatter that characterizes the experimental data makes it extremely difficult to derive a law that is able to accurately quantify this change of behaviour. A closer look at the experiments carried out over the years reveals that many parameters (as listed earlier) vary from test to test. Hence, although the experimental data are able to qualitatively describe the effect that the rate of the applied loading has on the prism behaviour/response, they are unable to accurately quantify this effect and to identify the causes of the gradual change exhibited in their structural response as described above. For this reason, resort is presently made to FE analysis in order to investigate in more detail the response of concrete under high rates of loading as influenced by these various parameters.

## 3. Material modelling of concrete

The material model presently adopted for describing the behaviour of concrete is fully defined by a single parameter (the uniaxial compressive strength  $f_c$ ) and does not rely on strain softening, stress-path dependency or loading-rate sensitivity, placing emphasis, instead, on the response of concrete to multiaxial (i.e. triaxial) stress conditions. Full details of the FE model can be found elsewhere [1,2].

## 4. Modelling of the dynamic problem

The structural form which provides the basis of this investigation is a concrete prism which is assumed to be fixed at its bottom face and to be subjected to an axial load applied at its upper face through a rigid element with the same cross-section (see Fig. 2) so that the external load is distributed uniformly on the upper face of the concrete prism (full bond at the interface of these

two elements is assumed). Both the concrete prism and the rigid element are modelled by using the 27-node Lagrangian brick element [4] which adopts a  $3 \times 3 \times 3$  integration rule. Meshes consisting of  $3 \times 1 \times 1$  and a  $1 \times 1 \times 1$  elements are adopted for the concrete prism and the rigid element respectively (see Fig. 2). The use of a sparse FE mesh contrasts with what other investigators have used previously for reasons fully outlined in ref. [1]. The mass of the specimen is modelled as concentrated masses distributed to all FE nodes.

There is considerable confusion in the literature as to how loading is applied, described and measured. There are several possibilities. *Average strain rate*: calculated as the average rate of displacement at the very top of the specimen divided by the length of the whole specimen. *Maximum value of average strain rate*: calculated at the section of the specimen with the largest value of average strain rate. *Mid-height strain rate*: evaluated at the mid-height region of the specimen. *Applied stress rate*: defined as the load increment applied in each time step divided by the cross-sectional area of the specimen and the length of the time step used.

## 5. The effect of the strain-rate measuring technique

In Fig. 3 a relationship is presented between  $\max P_d / \max P_s$  and strain rates evaluated by using different methods (i.e. average strain rate, maximum value of average strain rate, and mid-height strain rate). By comparing the three resulting relationships it is obvious that they are significantly different. The use of mid-height strain rate calculated in the mid-height region of the specimen may lead to misleading conclusions due to the fact that, for high rates of loading, only the upper part of the prism is affected and, therefore, the mid-height region exhibits less deformation, so that the strain rate calculated in this region is much less than the strain rate exhibited in the upper area of the specimen. Comparing these relationships with the experimental data in Fig. 3, it is obvious that the relationship between the  $\max P_d / \max P_s$  and the maximum value of average strain rate is the relationship that is closest to the experimental data.

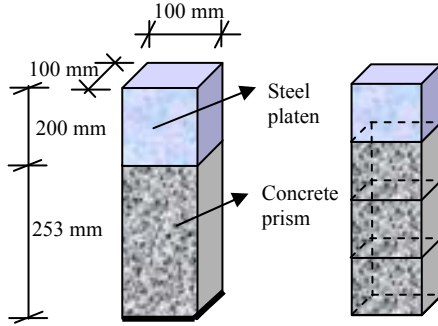


Figure 2. The specimen used for the investigation and FE model of the concrete prism under investigation.

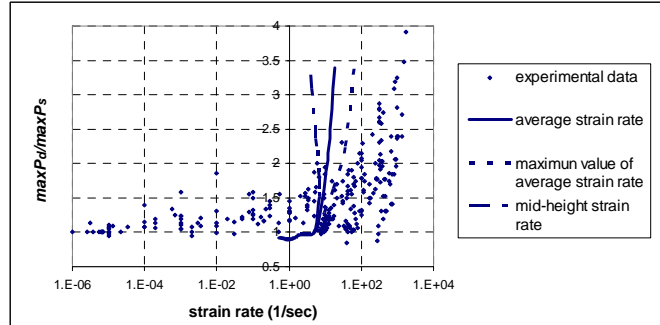


Figure 3. Relationship between  $\max P_d / \max P_s$  and differently evaluated strain rates and their comparison with experimental data.

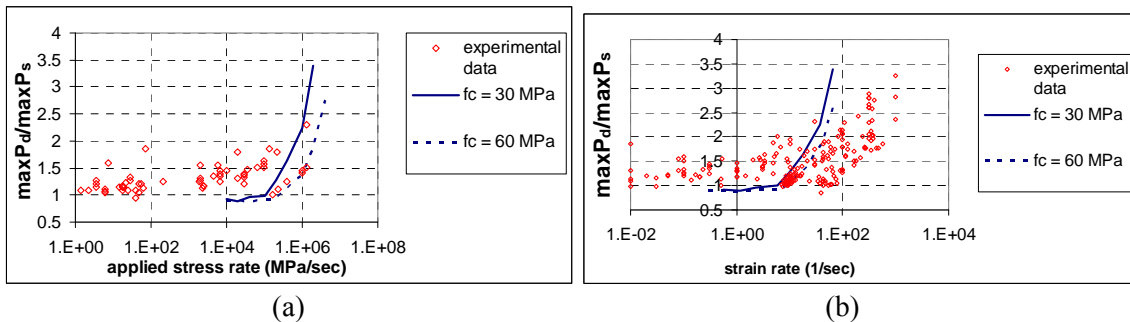


Figure 4. Numerical predictions and experimental data of specimen strength gain for varying  $f_c$ : (a) applied stress rate; (b) maximum value of average strain rate.

## 6. The effect of $f_c$

The majority of experimental investigations [2,5,6] indicate that, the higher the value of  $f_c$ , the lower the increase in the specimen strength becomes under high loading rates, but the significance of this effect varies depending on the experimental investigation. This conclusion is verified by the results obtained from the numerical investigation. The structural form used for this purpose consists of the concrete prism shown in Fig 2. The prism height is 253mm and its cross-section forms a square with a side of 100mm. The rigid element has the same cross-section but its height is 200mm. Two values of  $f_c$  are used in the present investigation: 30 MPa and 60 MPa. The results obtained for these two strengths are presented in Fig. 4 in the form of relationships between the increase of specimen strength  $\max P_d/\max P_s$  with (a) applied stress rate and (b) maximum value of average strain rate. In these figures, the numerical predictions are accompanied by the overall experimental data. The comparison of the results obtained from these case studies reveals that the specimens with the smaller  $f_c$  (30 MPa) exhibit a larger increase in strength with increasing rates of loading than that exhibited by the stronger specimen ( $f_c = 60$  MPa). This difference in the increase of strength between the weaker and stronger specimens becomes larger as the level of loading rate increases. Comparing the numerical predictions with the experimental data reveals that, although the variation of the value of  $f_c$  affects to some extent the behaviour of the concrete specimens, any such variations appear to be rather small since the effect of  $f_c$  seems to disappear within the much more pronounced scatter of the experimental data.

## 7. The effect of loading technique

In the past, many different experimental techniques (depending on the desired loading rate) have been used. In order to obtain an idea on how the different loading methods affect the experimental results, the latter are grouped into categories depending on the loading method used to apply the external load. The most commonly used loading methods are hydraulic (Fig. 5a), the drop-hammer (Fig. 5b) and the Split Hopkinson Pressure Bar (SHPB) (Fig. 5c) methods. Each of these groups of data is characterized by a scatter that may reflect the effect of parameters such as  $f_c$ , density, size and shape of specimen, etc. By observing the data depicted in Figs 5a to 5c, it appears that the use of different loading techniques may be significant factor contributing to the scatter that characterizes the experimental data. Thus, the results in Figs 5a and 5b are similar in that they indicate that the increase of the specimen strength commences at strain rates as low as  $10^{-5}$  to  $10^{-4}$   $\text{sec}^{-1}$  and gradually increases as the rate of loading becomes larger; furthermore, the scatter of the experimental data does not allow definitive conclusions to be drawn regarding the effect of the type of loading technique used on specimen behaviour. In contrast to the experimental data shown in Figs 5a and 5b, the results presented in Fig 5c, which were obtained from tests using the SHPB to apply the external load, show that the increase of the specimen's strength commenced suddenly at a strain rate of around  $10$   $\text{sec}^{-1}$  and beyond. For strain rates larger than  $10$   $\text{sec}^{-1}$  the increase in specimen strength is rapid as the rate of loading increases (and not gradual as in the previous cases). Furthermore, the SHPB experimental data is characterised by significantly less scatter than those of the other testing methods.

In order to investigate numerically the effect of the different loading mechanisms on the test scatter, two additional case studies are presented. In both cases the  $f_c$  used is 30 MPa. In the first case study, the external load is imposed in the form of displacement increments (instead of force increments) which are applied at the top face of the specimen. For the second case study, the external load is applied as an initial velocity. In order to achieve the latter, the rigid element situated on the top of the concrete specimen is assumed to have a concentrated mass of 20 kg, which is considerably larger than that of the specimen. This mass is assumed to have an initial velocity, the value of which varies depending on the desired loading rate. The results obtained

from the case studies are presented graphically in Fig. 6 in the form of relationships between the increase of strength  $\max P_d/\max P_s$  of the specimen with (a) applied stress rate and (b) maximum value of average strain rate. In all these figures, the numerical predictions are accompanied by experimental data so as to investigate the contribution of the loading-technique parameter to the overall scatter. The comparison of the numerical results shows that the method of loading has a relatively small effect on the increase in strength exhibited by the specimen under high rates of loading, so that the contribution of this parameter to the scatter of the experimental results would appear to be relatively modest.

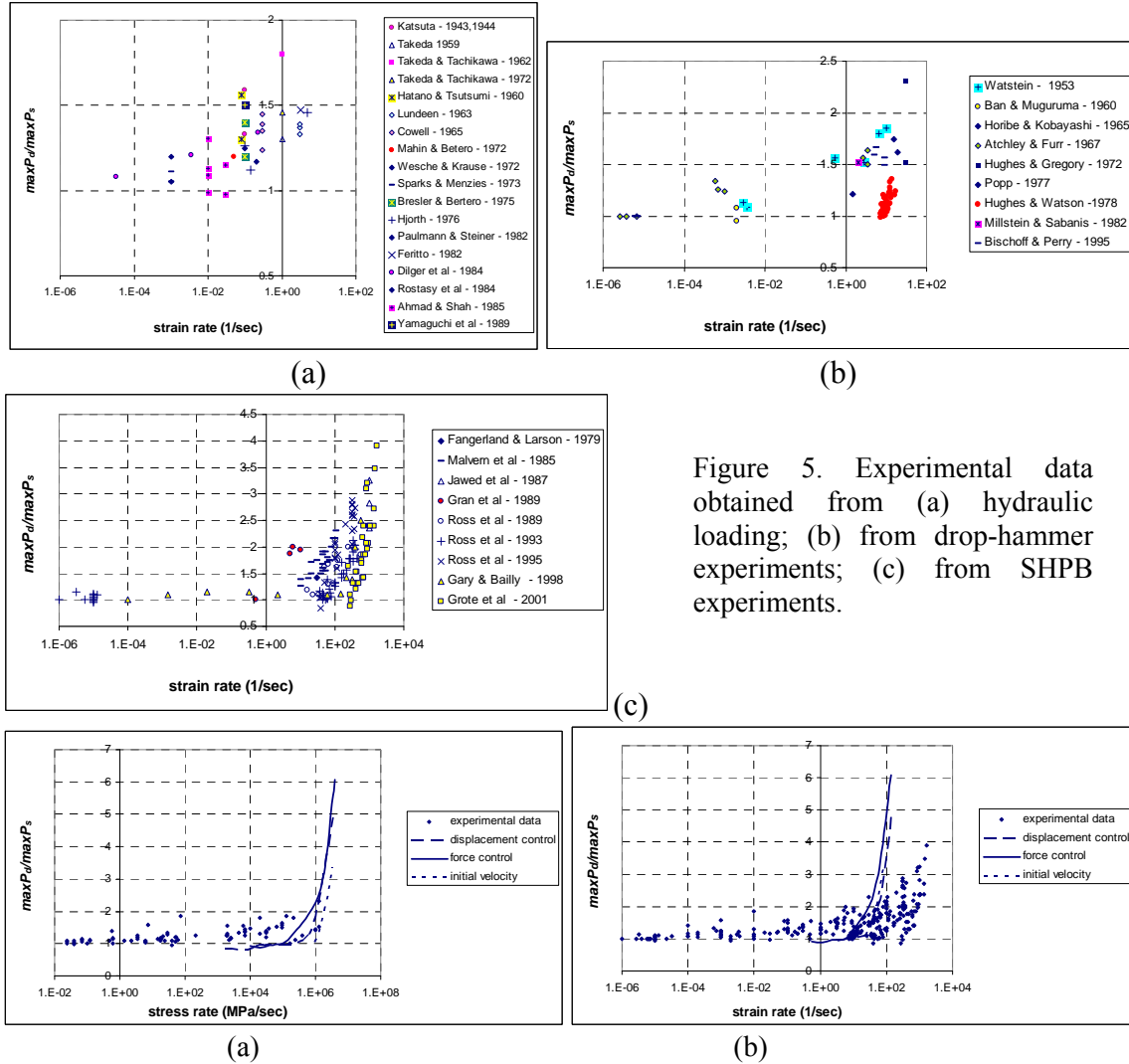


Figure 5. Experimental data obtained from (a) hydraulic loading; (b) from drop-hammer experiments; (c) from SHPB experiments.

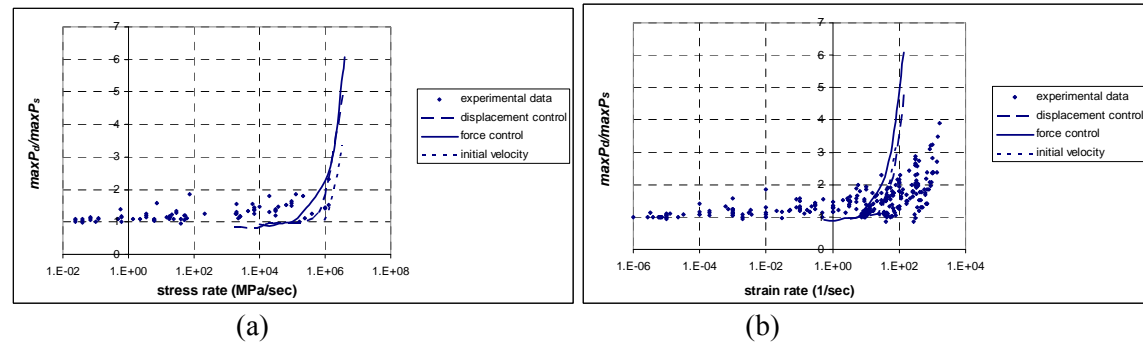


Figure 6. Numerical predictions and experimental data of specimen strength gain for different loading techniques: (a) applied stress rate; (b) maximum value of average strain rate.

## 8. The effect of size and shape of specimen

Other factors that could contribute to the scatter that characterizes the experimental data are the cross-sectional area and the length of the specimen. Changes in these two parameters lead to changes in the axial stiffness and mass that might play a significant role in specimen response under high loading rates. In viewing the experimental data presented in Figs 5a and 5b, one observed that they are characterized by significant scatter, while such experimental scatter is considerably less in Fig. 6c. This difference in scatter might be explained by the fact that,

whereas in the experimental investigations in which a drop-hammer or a hydraulic mechanism were used the size and shape of the specimens tested varied significantly, in the experiments which used the SHPB to apply the external load the specimens tested were similar in size (the cross-sectional area of the specimens is approximately the same as that of the pressure bar and their height is small). Refs [7,8] employed an SHPB to investigate cylindrical concrete specimens with different sizes under high rates of compressive loading. In the investigation of Malvern *et al* [7] the cylinder specimens had a diameter of 76 mm and a height of 76 mm, whereas in the investigations of Ross *et al* [8] the specimens had a diameter of 51 mm and a height of 51 mm. A comparison of the results obtained from the two investigations shows that the larger specimens exhibited much larger increases in strength beyond a certain loading rate. Moreover, the smaller specimens began to be affected by the loading rate at much higher levels of loading rate than the larger specimens. A similar conclusion was drawn by Ahmad and Shah [6] who, on the basis of experimental data, derived an analytical equation linking the strength of concrete specimens to the rate of loading (expressed as strain rate), the  $f_c$  of the concrete used and the height and cross-sectional area of the specimen which predicted that a reduction in the cross-sectional area or an increase of the height of the specimen results in a decrease of load-carrying capacity with the rate of loading.

In order to investigate numerically the effect of specimen cross-sectional area and length on specimen behaviour under high rates of loading, three additional specimens are now investigated. The specimens are similar to that shown in Fig. 3 except for the following changes. In the first case, the side of the cross-section of the specimen will be set to 50mm (instead of 100mm) in order to reduce the cross-sectional area to a quarter of that used originally. In the second case, the length of the specimen will be half of the original (126mm instead of 253mm). Finally, in the third case, both the side of the cross-section and the length of the specimen will be half of those in the original specimen. The numerical results obtained are presented graphically in Figs 7a and 7b in the form of relationships between the increase of strength  $maxP_d/maxP_s$  of the specimen with (a) applied stress rate and (b) maximum value of average strain rate. The numerical predictions in Figs 7a and 7b are also accompanied by the relevant experimental data.

By examining the results in Fig. 7a, it is apparent that the variation in the cross-sectional area and height has some effect on specimen response with increasing stress rate. In particular, it seems that the larger the cross-sectional area and the longer the specimen the larger the increase in strength becomes. However, these trends are less obvious in Fig. 7b, where the results suggest that the increase in strength exhibited by the various specimens is similar when variations with strain rates are considered. Therefore, by comparing the numerical predictions with the experimental data, it is evident that, although the variation of the specimens' height and cross-sectional area may have some effect on the dynamic response, such effect is practically lost within the experimental scatter.

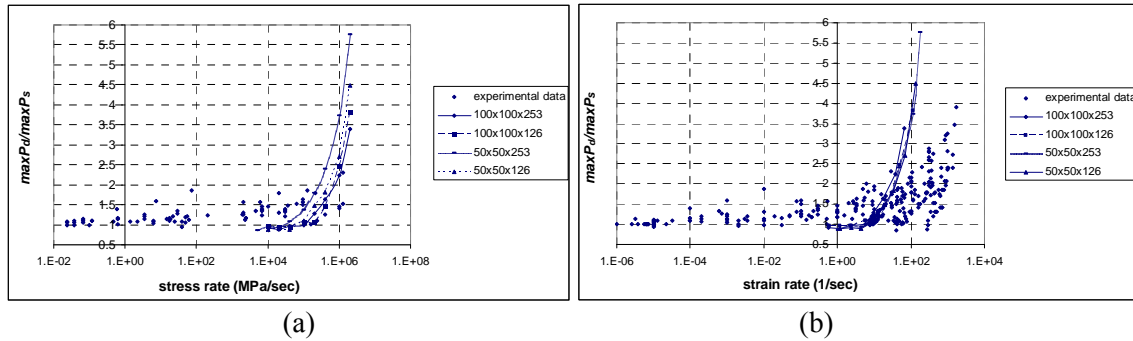


Figure 7. Numerical predictions and experimental data of specimen strength gain for different specimen sizes: (a) applied stress rate; (b) maximum value of average strain rate.



A further insight into the effect of the variation of specimen height and cross-sectional area is obtained by studying the results presented in Figs 8a and 8b which provide relationships of  $\max P_d/\max P_s$  with differently calculated strain rates for specimens with (a) one quarter of the original cross-sectional area (50x50x253) and (b) half the original height (100x100x126). Interestingly, the results suggest that, the shorter the specimen and the smaller the ratio between height and diameter ( $h/d$ ), the more uniform the distribution of the strain along its height becomes, as explained below. In the case of the specimen with a smaller cross-sectional area (50x50x253), the curve describing the relationship of  $\max P_d/\max P_s$  with the average strain rate at the mid-height region of the specimen is very different from the curves describing the relationship of  $\max P_d/\max P_s$  with the maximum value of the average strain rate and with the average strain rate (see Fig. 8a). This implies that the strain is not uniformly distributed along the height of the specimen. On the other hand, in the case of the shorter specimen (i.e the one with the smallest  $h/d$  ratio), the results presented in Fig 8b show that the differences between the same relationships are much smaller, suggesting a more uniform distribution of strain along the height of the specimen. Therefore, employing shorter specimens or specimens with smaller  $h/d$  ratios may in fact help reduce the effect of the different measuring techniques used to evaluate strain. This is confirmed by the experimental data presented in Fig 5c, where the test values obtained from SHPB experiments revealed that the smallest scatter was associated with the shorter specimens. Finally, whereas variations in cross-sectional area and height of specimens were found to have a relatively small effect on experimental-data scatter, a much more significant contribution to this overall scatter emerges from the different methods variously employed for calculating strain. Thus, it is obvious from the results presented in Figs 8a and 8b that, the bigger the height and the  $h/d$  ratios of specimens, the greater the differences in the values of strain calculated by using different methods.

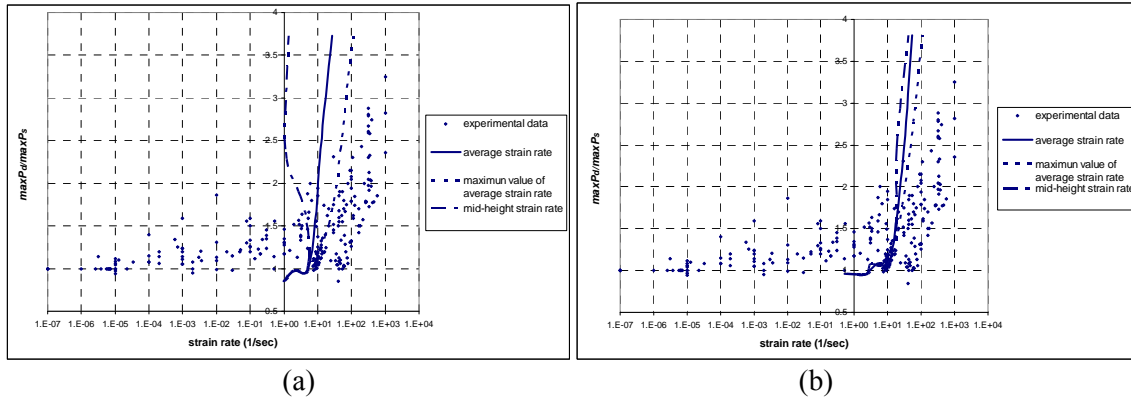


Figure 8. Numerical predictions and experimental data of specimen strength for varying specimen sizes and different methods for calculating strain rates: (a) specimen 50x50x253; (b) specimen 100x100x126.

## 9. The effect of specimen density

Another parameter that varies in experimental investigations is the density of the concrete specimen tested, as the use of different concrete mixes may result in a variation of this parameter. In order to investigate the effect of density variation, the structural form chosen in this investigation is the specimen shown in Fig. 3 but with the density of concrete ( $\rho$ ) now assumed to be 20% higher than that originally used (which was 2400 kg/m<sup>3</sup>). The numerical results for this prism, when subjected to high rates of uniaxial compressive loading, are presented in Figs 9a to 9b in the form of relationships between the increase of strength  $\max P_d/\max P_s$  of the specimen with (a) applied stress rate and (b) maximum value of average strain rate. The numerical predictions in these figures are also accompanied by experimental data, and it becomes evident

that, even the 20% increase in density assumed (quite large from a practical viewpoint), seems to have a small effect on specimen behaviour.

## 10. The combined effect of various factors

The parametric studies carried out so far investigated the individual effects of various factors on the behaviour of concrete prism specimens under high rates of uniaxial compressive loading. These studies revealed that, although the variation of each of these parameters, from one experimental investigation to another, do have a quantifiable individual effect on the results obtained, each individual effect on its own cannot account for the magnitude of the scatter that characterizes the experimental data. Therefore, the combined effect of varying all the different parameters studied earlier is now to be investigated. The values of these parameters are selected based on experience gained from the previous case studies. The aim is to select parameter values in such a way as to create two extreme (or “bounding”) case studies, which will lead to the largest and smallest possible strength increases  $\max P_d/\max P_s$  as the loading rate increases, thus providing upper and lower bounds to possible predictions. The results obtained are presented in Figs 10a and 10b in the form of curves expressing the increase of specimen strength with (a) applied stress rate and (b) maximum value of average strain rate. From these figures, it is possible to conclude that the combined effect due to the simultaneous variation of a number of parameters is much more significant for specimen behaviour than the individual effect of each parameter. This combined effect can be clearly observed in both figures, being largest when the strength increase is given as a function of applied stress rate and smallest (but still quite significant) when adopting the maximum value of average strain rate.

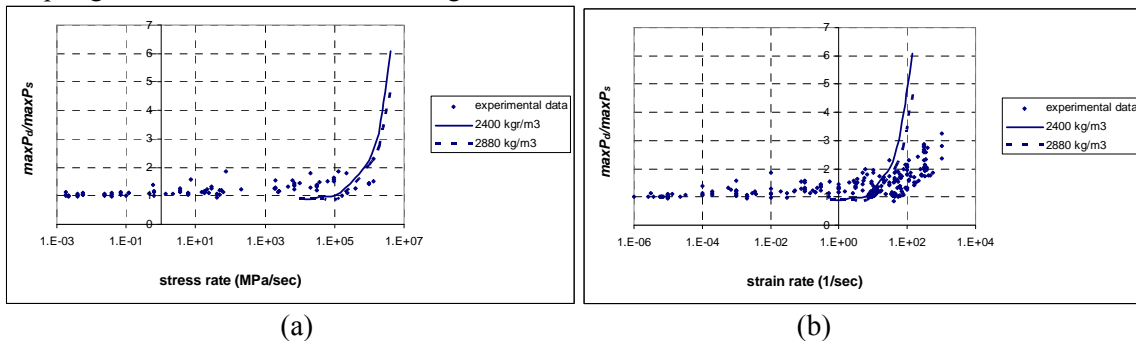


Figure 10. Numerical predictions and experimental data of specimen strength gain for varying concrete densities: (a) applied stress rate; (b) maximum value of average strain rate.

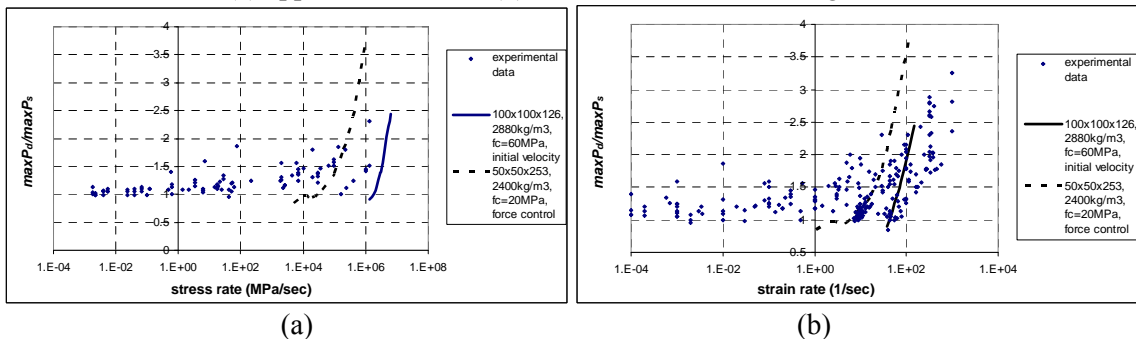


Figure 11. Numerical predictions and experimental data scatter of specimen strength gain for combined parameter variation: (a) applied stress rate; (b) maximum value of average strain rate.

## 11. Conclusions

Concrete specimens under dynamic loading cannot be used to describe concrete behaviour (as usually assumed) since, in contrast with static loading, they do not constitute a material unit from which average material properties may be obtained. Under dynamic tests, concrete specimens must be viewed as structures since their response is directly linked to the inertia effect of their mass (and, of course, boundary conditions) and the fact that the strains are not uniform along the height. Therefore, the use of experimental data from dynamic tests in order to develop constitutive models of concrete behaviour under dynamic loading is questionable.

Based on the data obtained from the numerical parametric investigations carried out, it can be concluded that the scatter caused by the individual effect of the variation of  $f_c$  of the concrete, the specimen cross-sectional area, its length, the loading technique or the density cannot account for the magnitude of the scatter that characterizes the available experimental data. However, the combined effect of a number of such parameters is much more substantial and is able to account for the scatter in the experimental data to a significant extent though not completely.

However, the full extent of the scatter can be explained if, in addition, one also allows for the different measuring techniques and strain definitions adopted over a century of testing. The experimental scatter is significantly reduced when the Hopkinson bar method is used in the tests, and this is confirmed by the present numerical analysis when the maximum value of the average strain rate (mimicking the Hopkinson bar experiment) is adopted. In the case of the specimen's height it was concluded that, the shorter the specimen, the more uniform the distribution of the axial strain along its height becomes, and this is the reason why the short specimen used in the Hopkinson bar experiments seems to provide the best experimental option to date. A more uniform distribution ultimately leads to less variation in the value of axial strain evaluated when using different measuring techniques. The present numerical investigation has proven that the use of different methods in evaluating strain is responsible for a substantial amount of scatter in the experimental data, as pointed out above. Thus, the shorter the specimen, the less the scatter produced due to the different strain-measuring methods. However, the results obtained from such specimens are heavily affected by the interaction between the loading mechanism (and, in particular, by the steel platens or the metal bars used to apply the external load) and the specimen itself.

## References

- [1] Kotsovos M.D., Pavlović M.N., *Structural Concrete: Finite-element analysis and design*. London: Thomas Telford, 1995.
- [2] Cotsovos DM. *Numerical Investigation of Structural Concrete under Dynamic (Earthquake and Impact) Loading*. PhD thesis, University of London, UK.
- [3] Bischoff PH, Perry SH. Compressive behaviour of concrete at high strain rates. *Materials & Struct.*1991;RILEM;**24**;425-450.
- [4] Bathe K-J. *Finite element procedures*. Prentice-Hall;New Jersey;1996.
- [5] CEB. Concrete structures under impact and impulsive loading. *Synthesis Report, Bulletin d'Information No. 187*, Comité Euro-International du Béton, Lausanne; 1988.
- [6] Ahmad SH, Shah P. Behaviour of hoop confined concrete under high strain rates. *ACI Journal* 1985;**82**:634-647.
- [7] Malvern LE, Tang T, Jenkins DA and Gong JC. Dynamic compressive testing of concrete. In *Proc. 2<sup>nd</sup> Symposium on the Interaction of Non-Nuclear Munitions with Structures*;US; Department of Defence;Florida; 1985;119-138.
- [8] Ross CA, Jerome DM, Tedesco JW, Hughes LM. Moisture and strain effects on concrete strength. *ACI Mat. Journal* 1996;**93**:293-300.